

Paving the Path for a New Generation of High-Efficiency Supermarket Refrigerated Display Cases

*Rafik Sarhadian, Ramin Faramarzi, Bruce A. Coburn, and John Lutton,
Southern California Edison
Hodayun Navaz, Kettering University
David Walker, Foster-Miller Inc.*

ABSTRACT

This paper discusses the results of experimental evaluation of a number of viable and near-term energy-efficiency solutions applicable to open vertical refrigerated display cases. With energy usage intensity of 43 kWh to 70 kWh per square-foot per year, supermarkets are one of the most energy-intensive commercial building types in the United States. A major factor affecting the design and operation of supermarket refrigeration systems is the cooling load requirements of the display cases. Medium-temperature display cases and, in particular, open vertical display cases, are one of the most thermally vulnerable display cases in supermarkets. These display cases, which are typically used to merchandize meat, dairy and delicatessen, fish and produce, operate at discharge air temperatures of 28°F to 32°F. They also comprise the largest portion of display case line ups. Historically, display case manufacturers have not invested in energy-efficiency improvements of their products. This has been due to lack of demand from their customers as well as first cost considerations. Furthermore, the absence of energy-efficiency standards for display cases, coupled with supermarkets' dominant emphasis on merchandising facets have impeded the related research and development efforts.

Laboratory tests were conducted to quantify the impacts of several energy-efficiency measures on the performance of a selected open vertical display case. The result of incorporating these technologies indicated an improvement of 19% in refrigeration effect and reduction of 11% in electric power usage of the refrigeration system (excluding condenser). These improvements were achieved without affecting the target product temperature.

Introduction

This work was sponsored in part by the United States (U.S.) Department of Energy, Office of Building Technology, State and Community Programs under contract DE-AC05-00OR22725 with UT-Battelle, LLC. The purpose of this project was to evaluate the impacts of near-term energy-efficiency solutions in refrigerated display cases without affecting food safety or hampering the merchandizing facets. The project employed a combination of experimental and analytical methods to evaluate the effects of selected viable technologies on the energy-efficiency of a thermally vulnerable display case. The economics of these near-term technologies can have an influential role in their market adoption. The study, however, temporarily steered away from considering potential cost barriers and focused on technical feasibility and energy impacts.

Background

In the U.S. today, over 199,000 supermarkets operate their refrigeration systems continuously to ensure proper merchandizing and safety of their perishable food products (Food Marketing Institute 2004). Supermarkets are one of the most electric energy intensive commercial building types in the U.S. Their annual electric energy usage intensity is between 43 kWh to 70 kWh per square-foot (Komor et al. 1998). In a typical supermarket, refrigeration of perishable foods accounts for about 50% of total electric energy usage (ADL 1996). Furthermore, past research reveals that the major contributor to the total cooling load of medium-temperature open vertical display cases is the infiltration load, which comprises roughly 70% to 80% of the total cooling load. Infiltration load refers to the entrainment of warm and moist air from the room into the refrigerated space (Faramarzi 1999). These cases have a large presence in supermarkets and account for up to 50% of the total refrigerated display case line ups (Electric Power Research Institute 1992).

Approach

This study has been categorized into three phases. A brief description of each phase is provided below. The testing of the display cases followed the procedures specified in the American Society of Heating, Refrigerating and Air-Conditioning Engineers (*ASHRAE Standard 72-98* (ASHRAE 1998)).

In phase 1, the energy impact of a number of viable display case energy-efficiency measures (EEMs) was quantified by performing whole-building hourly simulations. A special version of the U.S. Department of Energy's (DOE-2) program was used to develop a model based on an actual supermarket information. The model was then calibrated using available end-use monitored data to increase confidence in simulation results. As part of the calibration process, the non-weather dependent electrical loads, such as lighting and equipment as well as their corresponding hourly usage profiles were reconciled with the end-use monitored data. Simulation results were used to identify viable energy-efficient technologies for implementation in the second phase of the project. Additionally, under this phase, a standard eight-foot long, medium temperature open vertical display case was selected and evaluated for thermal performance benchmarking purposes. These cases are typically used for merchandizing poultry, fish, produce, fresh meat, dairy and delicatessen items and have a large presence in supermarkets. Thermal characteristics of the selected standard display case were evaluated in the laboratory to establish baseline performance data. Finally, a combination of analytical and experimental methods was used to study the air curtain performance. These methods involved the use of digital particle image velocimetry (DPIV) and laser Doppler velocimetry (LDV) to visualize and quantify the air flowfield along the plane of the air curtain. The DPIV and LDV results were also used to calibrate a computational fluid dynamics (CFD) model, which was later used to simulate the air curtain performance for a variety of conditions.

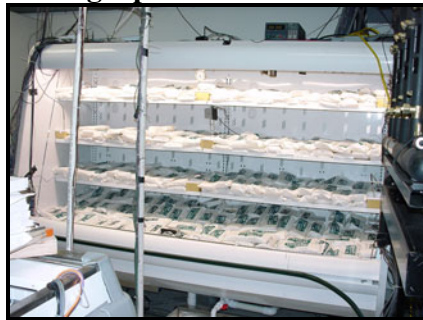
In phase 2, the baseline display case was retrofitted with the selected energy-efficient technologies, which were identified in phase 1. Results obtained from CFD modeling were used to determine the best discharge air grille (DAG) configuration and velocity profile to minimize the infiltration load of the display case. Based on the obtained intelligence, limited modifications were made to the geometry of DAG assembly. The thermal performance of the display case was then evaluated.

In phase 3, findings from previous phases were used to develop energy-efficiency specifications for fabricating a new display case (prototype). The shell of the prototype case was fabricated with a modified DAG configuration with the intention of reducing the infiltration load of the case. The next step included the design, fabrication and installation of the energy-efficient components. These components included: low temperature differential evaporator, tangential evaporator fans driven by an electronically commutated motor (ECM), high-efficiency super T8 fluorescent lamps with high power factor ballast, dual-port thermostatic expansion valve (TXV) and micro-channel liquid-to-suction heat exchanger (LSHX). Lastly, the thermal performance of the prototype was evaluated.

Baseline Display Case Description

The eight-foot long baseline display case with the rated cooling capacity of 1,561 Btu/hr per foot was equipped with four shelves, three shaded pole fan motors, and two rows of standard T8 canopy lights with electronic ballast (Figure 1). Off-cycle defrost was initiated three times per day and terminated at coil outlet temperature of $\sim 47^{\circ}\text{F}$. Following the manufacturer's published data, the baseline display case was set up to operate at a saturated evaporating temperature (SET) of 17°F and discharge air temperature (DAT) of 28°F (Hill Phoenix 2001).

Figure 1. Photograph of the Baseline Display Case



Cooling Load Constituents

The total cooling load of a display case is comprised of both sensible and latent portions. Generally, the sensible portion is comprised of heat gained from lights, evaporator fan motors, defrost process (electric or hot gas), anti-sweat heater(s), thermal conduction, radiation, warm air infiltration and product pull-down load. The latent portion, on the other hand, is comprised of moist air infiltration and product latent heat of respiration (ASHRAE 2002). A display case heat transfer model was developed to determine the contribution of various cooling load components based on the measured data. Figure 2 depicts test data representing the main cooling load components for a medium-temperature, open, multi-deck display cases (Faramarzi 1999).

Energy-Efficiency Measures (EEMs)

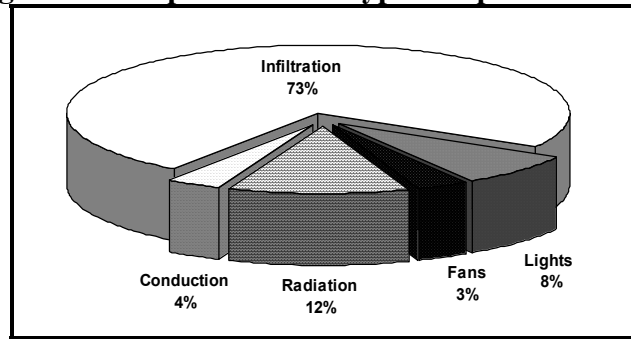
The selection of the EEMs in this study was performed based on the following criteria:

1. Near-term implementation

2. Potential for energy-efficiency improvements
3. Enhancement of the ability to maintain target product temperature

The selected EEMs were grouped into five main categories. Technologies within these categories were expected to improve the refrigeration system performance, maintain a tightly targeted product temperature and reduce the electric power usage of the case.

Figure 2. Cooling Load Components of a Typical Open Multi-Deck Display Case



EEMs Descriptions and Categories

1. *The evaporator coil assembly EEM* consisted of a high-efficiency evaporator coil and a dual port TXV. The high-efficiency coil features a large heat transfer surface with staggered fin design, and enhanced tubing. Table 1 compares the key operational characteristics of the high-efficiency and baseline evaporator coils. The dual-port TXV regulates the refrigerant flow by opening its larger port during post-defrost periods and reducing the flow through its smaller port for temperature holding.

Table 1. Summary of Baseline and Prototype Case Evaporator Specifications

Design Parameter	Baseline Evaporator	Prototype Evaporator
Overall Dimensions	81"W x 7 5/8"H x 12" D	81"W x 7 1/2"H x 13 9/16" D
Number of Circuits	4	6
Number of Tube Passes per Circuit	12	12
Liquid Line Fed	Front	Back
Number of Fins per Inch	2	3 for 5 Front Rows 4 for 7 Rear Rows
Fin Material	Flat Aluminum	Flat Aluminum
Tube/Pipe Outside Diameter	9/16"	3/8"
Tube/Pipe Material	Copper	Copper
Tube/Pipe Internal Surface	Smooth	Enhanced

2. *The air distribution EEM* consisted of two tangential fans (Figure 3a) operated by a 1/3 horsepower dual shaft ECM, which had an efficiency of about 80%. Each tangential fan had 30 blades with an airflow inlet/outlet angle of 180 degrees. The wheel diameter and length of each tangential fan was 4.5" and 36", respectively.

3. The liquid-to-suction heat exchanger EEM was made of aluminum and utilized micro-channel heat exchangers (Figure 3b). In each module a liquid channel was sandwiched by 12 vapor tubes. These vapor tubes were 5/32" in diameter and 38" long. The liquid channel dimensions were: 3/32"D x 1.57"W x 40"L. The measured heat exchanger effectiveness, defined as the ratio of actual to maximum possible heat transfer, was about 70%.

Figure 3. Photographs of the Tangential Fans and LSHX



(a) Tangential Fans



(b) LSHX

4. The lighting system EEM consisted of high-efficiency super T8 fluorescent lamps (30 watts, 4100K) with low ballast factor electronic ballast (EB). The low ballast factor allowed the lamps operation at lower amperage. The power factor of the EB was over 90% with an input voltage of 120V and line current of 0.79A.

5. The air curtain EEM involved the investigation of the air curtain effectiveness in reducing infiltration load and maintaining the food products at a prescribed temperature. The investigation also identified those parameters that can have significant impact on the reduction of entrained air and infiltration rate. The analysis employed a combination of numerical and experimental methodologies to ascertain the thermo-fluid characteristics of air curtain and to better understand the entrainment phenomenon.

The experimental approach relied on the DPIV technology, which is based on a two-dimensional mapping of the flowfield within the air curtain. The velocity flowfield obtained from the DPIV was used to determine the volumetric rate of entrained air into the display case. Since determining the air velocities at the DAG and return air grille (RAG) were critical operational aspects of the air curtain, special attention was given to this measurement. For this reason, the highly accurate and non-intrusive technique of LDV was employed for precise determination of the discharge air velocity (DAV) and the case volumetric flow rate.

The numerical approach relied on CFD modeling of the display case. A CFD model was developed and calibrated using the experimental data in order to perform air curtain simulations. The boundary conditions of the CFD model were established based on the DAG and RAG velocity profiles obtained from the DPIV results. The CFD model was then used to perform a series of parametric simulations correlating the entrainment rate to key operational variables such as turbulence intensity and Reynolds number.

Test Design and Setup

The test setup and design followed guidelines specified in *ASHRAE Standard 72-98*. The refrigeration system was charged with a hydrofluorocarbon refrigerant (R-404A). The refrigeration system controller maintained a fixed saturated condensing temperature (SCT) of 95°F ($\pm 0.5^\circ\text{F}$) for all tests. The display cases were tested in a controlled environment room at

Southern California Edison's Refrigeration and Thermal Test Center (RTTC) located in Irwindale, Calif.

All tests were performed under steady-state conditions following *ASHRAE Standard 72-98*. Average DAT, which was the critical control point was maintained at 30°F ($\pm 0.5^\circ\text{F}$) to prevent the maximum product temperature from exceeding 41°F. The controlled environment chamber was maintained at a constant dry bulb (DB) temperature of 75.2°F $\pm 2^\circ\text{F}$ and wet bulb of 64.4°F $\pm 2^\circ\text{F}$, corresponding to 55% relative humidity (RH), throughout the entire 24-hour test period. The intensity of ambient lighting in the controlled environment room was 115 foot-candles and was in compliance with the ASHRAE standard, which requires a minimum of 74.4 foot-candles. The foot-candle measurement was taken at a distance of one foot from the air curtain. The entering liquid refrigerant temperature and pressure, measured at 6.1" of pipe length from the display case, were maintained at 80°F and 214 psig (corresponding to a SCT of $\sim 94^\circ\text{F}$). These parameters meet the ASHRAE standard, which requires the entering liquid temperature be 80.6°F $\pm 5^\circ\text{F}$, and SCT to be maintained between 89.6°F and 120.2°F.

The product temperatures were monitored at 24 locations within the display case. For each display shelf, two product simulators were located at the left end, the right end and the center. At each left, right, center location, one product simulator was placed on the shelf surface at the front of the shelf and one at the rear edge of the shelf. As a result, six product simulators were used on each of four shelves.

ASHRAE 72-98 also requires food product zones be filled with test packages and dummy products to simulate the presence of food product in the cases. According to the ASHRAE standard, food products are comprised of 80% to 90% water, fibrous materials, and salt. Therefore, plastic containers completely filled with a sponge material soaked in a 50% $\pm 2\%$ by volume solution of propylene glycol and distilled water were used to simulate the product during the tests. The spaces in the test display case where temperature measurement was not required were stocked with dummy products to stabilize the temperature in the case and account for transient heat transfer effects.

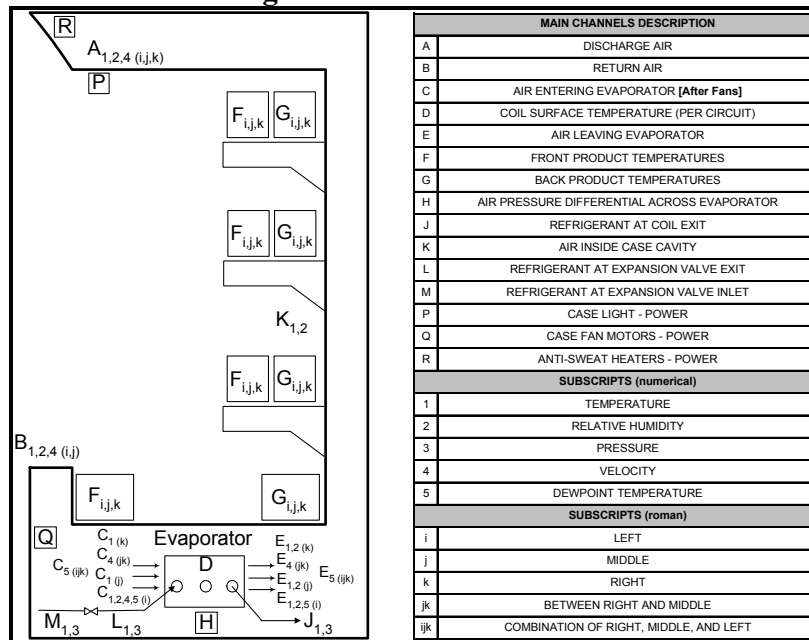
Data Acquisition

The RTTC's data acquisition system was set up to scan 128 data channels in ten-second intervals and to log channel outputs in two-minute intervals. Collected data was screened closely to ensure the key control parameters were within acceptable ranges. In the event that any of the control parameters fell outside acceptable limits, the problem was flagged and a series of diagnostic investigations were carried out. Corrections were then made and tests were repeated as necessary. Once the data passed the initial screening process, it was imported to RTTC's customized refrigeration analysis model where detailed calculations were performed. The collected data points from the two-minute intervals were averaged into hourly values where necessary and used for a secondary screening of the results.

Prior to the test, all instruments including thermocouples, resistance temperature devices, pressure transducers, anemometers, mass flow and power transducers, were calibrated. With the objectives of minimizing instrument error and maintaining a high level of repeatability and accuracy in the data, careful attention was paid to the design of monitoring system. The location of sensors within the test display case is depicted in Figure 4. The instrumentation was set up based on the following guidelines:

1. Use of sensors with high accuracy
2. Minimization of sensor drift errors by use of redundant sensors
3. Utilization of National Institute of Standards and Technology calibrated instruments of high accuracy
4. Elimination of interference from power conductors and high frequency signals by shielding sensor leads

Figure 4. Sensor Locations



Test Facility

The RTTC is a 3,800 square-foot testing facility. This facility is comprised of three main categories of test chambers: supermarket test chambers, HVAC test chambers, and refrigerated walk-in test chambers.

The supermarket test area is comprised of a controlled environment room and a mechanical room. In the mechanical room, three refrigeration racks and a variety of heat rejection equipment can serve various display case systems, which are housed in the controlled environment room. The controlled environment room is an isolated thermal zone served by independent cooling, heating and humidification systems. This allows simulation of various indoor conditions of a supermarket. The sensible cooling load representing people and other heat gain sources is provided by a constant volume direct expansion system, which reclaims waste refrigeration heat via a six-row coil. Auxiliary electric heaters located down-stream of the heat reclaim coils provide additional heating when required. While the air is conditioned to a desired thermostatic set point, an advanced ultrasonic humidification unit introduces precise amounts of moisture into the air surrounding the display cases. This moist air represents the latent load due to outside air and people. There are three laminar diffusers in the room, each supplying air at approximately 370 cubic-feet-per-minute.

Discussion of Results

This section discusses and compares results obtained from testing of the baseline and the prototype display cases. One of the critical challenges of the study was to maintain an identical maximum product temperature, while keeping average DAT at 30°F ($\pm 0.5^\circ\text{F}$) for both units. The warmest product temperature for both units was 39.6°F ($\pm 0.5^\circ\text{F}$), which was observed at the bottom shelf front center location and occurred during post-defrost periods.

The refrigeration system, test chamber, and the product temperatures were allowed to reach a steady-state equilibrium condition prior to initiation of the test runs. Figure 5 illustrates that the test chamber maintained relatively non-varying DB and RH during the entire test period for both units.

Figure 5. Two-Minute Room Dry-Bulb and Relative Humidity Data over 24-Hour Period

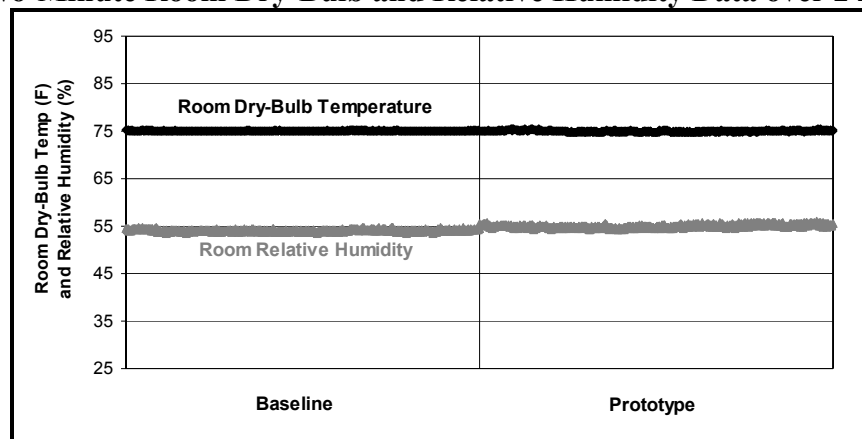


Figure 6 depicts the discharge and suction pressures for both display cases. The test rack controller was programmed to run at a fixed discharge pressure of 220 psig, corresponding to 95°F SCT, for both test scenarios. For the baseline unit, the suction pressure was set according to the case manufacturer's specifications to provide a SET of 17°F. For the prototype unit, the SET (or the suction pressure) was raised until a similar DAT and maximum product temperature as the baseline were achieved. As a result, the prototype case operated at a SET of roughly 23°F, which was about 6°F (or 8 psig) higher than the baseline case.

Discharge Air Temperature and Product Temperatures

The average DAT for both the baseline and prototype cases was about 30°F ($\pm 0.5^\circ\text{F}$) while maintaining an average product temperature of 33°F (Figure 7). The highest product temperature for both scenarios was recorded during post-defrost periods while the lowest was prior to initiation of defrost. The variations in product temperature can be attributed to variations in DAT. The DAT reached its lowest temperature at the beginning of the refrigeration periods due to frost or ice having been removed from the coil during defrosts. Unlike the prototype case, the DAT of the baseline tends to increase almost half way through refrigeration cycles. This increase can be attributed to larger frost formation on the baseline coil as a result of longer refrigeration periods.

Figure 6. Two-Minute Suction and Discharge Pressures Data over 24-Hour Period

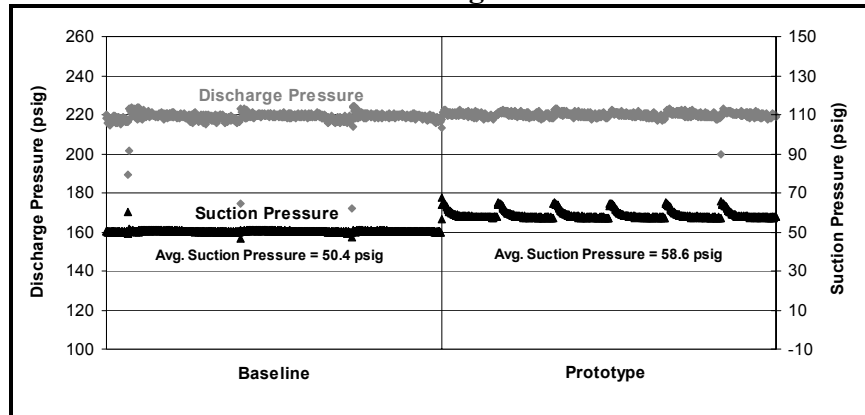
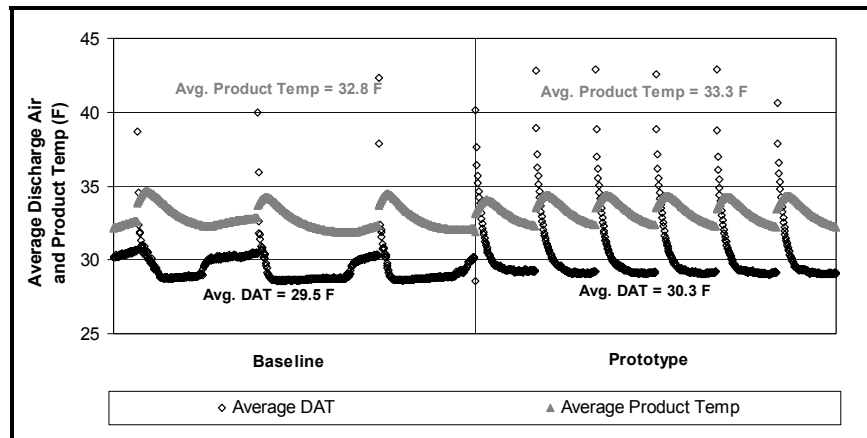


Figure 7. Two-Minute Average Discharge Air Temp. and Product Temperature Data over 24-Hour Period

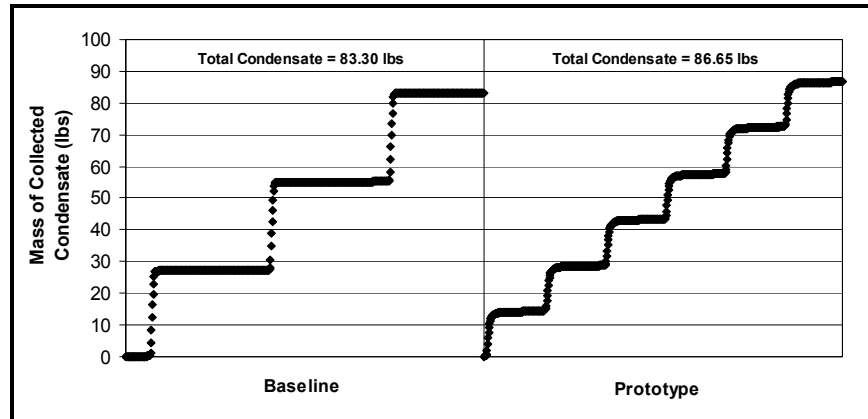


Collected Condensate and Defrost Duration

Figure 8 depicts the two-minute profile of condensate mass collected over the entire test period for both display cases. As shown, the overall magnitudes of collected condensate were relatively close for both scenarios. Horizontal lines in Figure 8 show no (or insignificant amount of) moisture being collected during refrigeration periods. Vertical lines indicate the mass of melted frost collected during each defrost cycle.

The defrost frequency for the baseline case was set to three defrosts per day (based on the manufacturer’s specifications), which resulted in 102 minutes of defrost over 24-hours. With only three defrosts per day, the more effective evaporator of the prototype case experienced faster frost blockage due to its higher rate of moisture removal than the baseline. As a result, after conducting a series of experiments, the optimum number of defrost cycles was set to six per day to minimize the adverse post-defrost product temperature rise. Doubling the number of defrost cycles in the prototype case increased the overall defrost duration to 168 minutes.

Figure 8. Two-Minute Mass of Collected Condensate Data over 24-Hour Period



Air Curtain Study

The CFD results of the air curtain study suggested that DAV characteristics including velocity profile, Reynolds number and turbulence intensity all have significant impacts on infiltration. The CFD model predicted the lowest entrainment rate to take place under conditions where the velocity profile at the DAG resembled a skewed parabola and the Reynolds number was around 3,000. Accordingly, several attempts were made to modify the DAG assembly to establish similar conditions as suggested by the CFD results. Unfortunately, none of these modifications proved to yield sizable reductions in the infiltration rate.

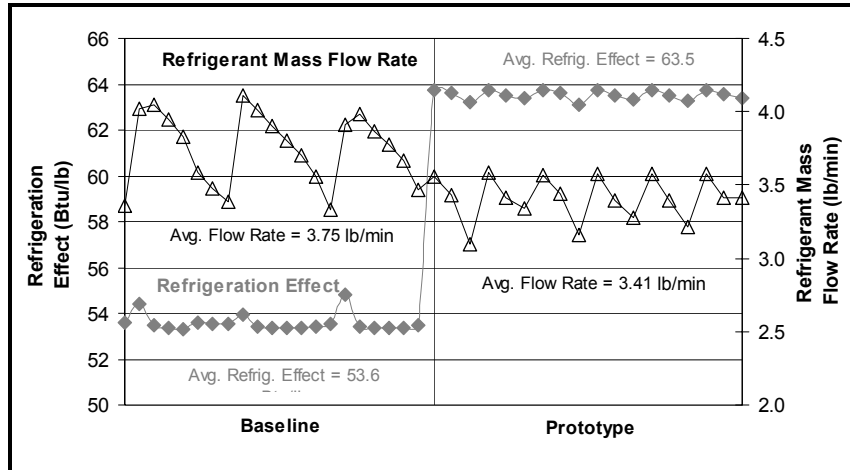
Evaporator Coil Effectiveness, Superheat, and Total Subcooling

The evaporator effectiveness as a function of the product of overall coefficient of heat transfer and its surface area (UA) for the prototype unit was improved by 68% over the baseline case. Use of a micro-channel LSHX resulted in roughly a 34°F increase in total system subcooling. The prototype case used a dual port mechanical TXV. This allowed for faster temperature recovery than in the baseline case during post-defrost periods. It also allowed for more effective utilization of the evaporator by operating at 6°F superheat, which was 4°F less than the baseline.

Refrigeration Effect and Refrigerant Mass Flow Rate

Figure 9 depicts the refrigeration effect and refrigerant mass flow rate for both cases. Refrigeration effect represents the cooling capacity of the evaporator per pound of refrigerant flow. The prototype case was operated at 63.5 Btu/lb, which was 10 Btu/lb (or 18%) higher than the baseline. This improvement was largely due to the use of a more effective evaporator, which allowed for operations at higher SET. A high-efficiency LSHX, which increased subcooling from 17°F to 52°F also made a partial contribution to the improvement in the refrigeration effect. The prototype case also required 9% less circulation of refrigerant than the baseline, which was a result of an improved refrigeration effect and a small reduction in cooling load.

Figure 9. Two-Minute Refrigeration Effect and Refrigerant Mass Flow Rate Data over 24-Hour Period



Cooling Capacity and Cooling Load Components

The cooling capacity, which is the product of refrigeration effect and mass flow rate, was 12,038 Btu/hr and 12,977 Btu/hr for the baseline and the prototype, respectively. The total cooling load was comprised of infiltration, radiation, conduction, and internal loads (lights and evaporator fans). As expected, the largest component of the cooling load was infiltration, which contributed over 80% to the total cooling load for each display case. Based on the heat transfer model's results, the contribution of radiation (8%) and conduction (4%) to the total cooling load remained unchanged since both display cases operated at similar average DAT. The contribution of internal loads, however, decreased from 6% in the baseline case to 5% in the prototype. This reduction was due to less heat dissipation from the high-efficiency lighting system and the evaporator fan motor.

Power, Energy, and System Efficiency

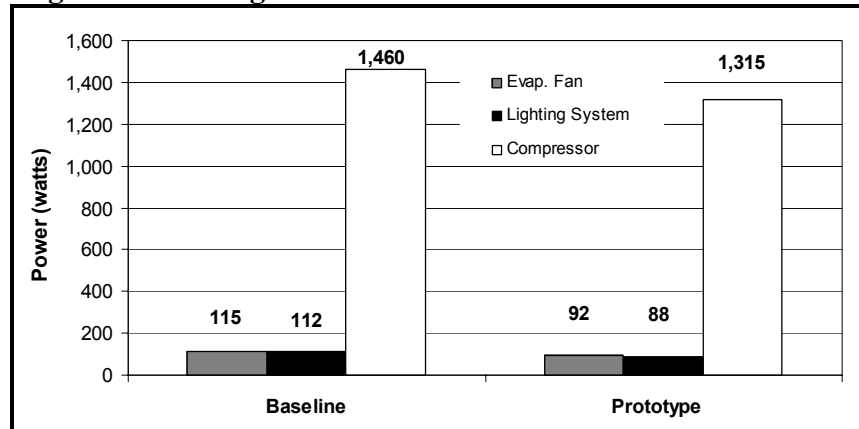
The prototype unit required roughly 20% less fan and lighting power than the baseline unit (Figure 10). Furthermore, the increase in refrigeration effect and decrease in refrigerant mass flow resulted in a drop of 10% in the compressor power requirement of the prototype case. Combining the savings obtained from the compressor, evaporator fan motor and lighting yielded 11% reduction in total power consumption and a 22% increase in the total energy-efficiency ratio (EER). Additionally, the decrease in compressor power run time of the prototype case translated into a savings of 14% in compressor energy usage.

Conclusions

Overall, the prototype display case operated more efficiently than the baseline. Despite several attempts to implement air curtain improvements, the infiltration load of the prototype display case remained the same as the baseline. Both the baseline and the prototype cases experienced a maximum post-defrost product temperature of 39.6°F ($\pm 0.5^\circ\text{F}$) at the bottom shelf front center location. The prototype evaporator coil UA was improved by 68% over the baseline

case. While the mass flow rate of refrigerant for the prototype decreased by 9%, its refrigeration effect was increased by 19% over the baseline case. The prototype unit benefited from a reduction of 10% and 14% in compressor power and energy consumption, respectively. Further power enhancements were made possible through efficient lighting (21%) and an efficient evaporator fan motor (20%). The overall impacts of all these measures resulted in a 22% improvement in the overall system EER. These improvements were achieved while target product temperatures were maintained and the total cooling capacity was similar to the baseline case. Future research is highly recommended to further investigate the air curtain performance and subsequently develop effective means to reduce infiltration.

Figure 10. Average End-Use Power Data over 24-Hour Period



References

- American Society of Heating, Refrigerating and Air-Conditioning Engineers (ASHRAE). 2002. *Refrigeration Handbook*.
- American Society of Heating, Refrigerating and Air-Conditioning Engineers (ASHRAE). 1998. Standard 72-1998. *Method of Testing Open Refrigerators*.
- Electric Power Research Institute (EPRI). 1992. *Field Testing of High-Efficiency Supermarket Refrigeration*, TR-1002351, December.
- Faramarzi, R. 1999. *Efficient Display Case Refrigeration*. American Society of Heating, Refrigerating and Air-Conditioning Engineers (ASHRAE) Journal. November, pp.46-54.
- Food Marketing Institute, Inc. (FMI). 2004. *Facts and Figures*. Retrieved from World Wide Web at <http://www.fmi.org/facts&figs/superfact.html>.
- Hill Phoenix. 2001. Merchandisers Engineering Reference Manual. Rev. 1: July, p. 134.
- Komor, P., C. Fong, and J. Nelson. 1998. *Delivering Energy Services to Supermarkets and Grocery Stores*. E Source. Boulder, Co. June.
- Arthur D. Little, Inc. (ADL). 1996. *Energy Savings Potential for Commercial Refrigeration Equipment – Final Report*, prepared for United States Department of Energy, Building Equipment Division Office of Building Technologies.